Tuijin Jishu/Journal of Propulsion Technology
ISSN: 1001-4055
Vol. 44 No. 5 (2023)

Optimization of Abrasive Water Jet Machining Parameters for Improved Surface Quality and Material Removal Rate in Stacking Composite

[1] Sridhar Akarapu, [2]Dr. P. Ramesh Babu

[1] Research Scholar, Department of Mechanical Engineering, Osmania University, Hyderabad
[2] Sr. Professor, Department of Mechanical Engineering, Osmania University, Hyderabad,

Abstract: This research presents the machinability of a hybrid steel mesh/basalt fiber/jute fiber stacked composite under abrasive water jet machining (AWJM), an experimental analysis based on the design of experiments is carried out in this work. Hybrid steel mesh/basalt fiber/jute fiber stacked composites were fabricated using a vacuum-assisted resin transfer molding (VARTM) process. The objective of this study is to investigate a relationship between abrasive pressure, traverse rate, abrasive amount rate, and nozzle distance in order to evaluate the surface roughness, kerf angle, and material removal rate of a Stacking composite (SC) made of Steel mesh, basalt fiber, and jute fiber (WBJBJW). The impact of each parameter on the result was evaluated using the Analysis of Variance (ANOVA) approach. To obtain a reduced surface roughness, kerf angle, and a better material removal rate, the process parameters were optimized using the desirability optimization technique. The experimental interpretations were carried out using the L29 Central Composite Design (CCD). The statistical method was used to assess the impact of each unique AWJC element. It was revealed that the aqua jet pressure had the greatest impact on the rate of material removal and surface roughness. The SR and KA, which decreased by 10.81% and 50.36% as the AJP strengthened at 300 MPa, were found to be influenced by the AWP. The desirability analysis (DA) optimises the AWJC characteristics of the (WBJBJW). It was discovered that the AWP had an impact on the SR and KA, which reduced by 10.81% and 50.36% when the AJP increased at 300 MPa. Results of SR, KA, and MRR values predicted by the RSM are evaluated using experimental data, showing that they agree with one another with minimal or no error.
Keywords: Steel mesh; Basalt; Jute; Abrasive; Roughness; Kerf angle; Desirability.

1. Introduction

The Stacking composite (SC) is a composite material consisting of interlaced fiber layers and metal sheets that has gained popularity in the structural parts of industries like aviation, marine, and automobile due to its properties, including lightweight, high specific strength, corrosion protection, and impact resistance, which outperform monolithic materials. Over time, researchers and structural designers have created several SC designs by interlacing various fibers such as Glass, Aramid, Carbon, and more, either between Steel mesh or Aluminum metal sheets or sandwiched with metal sheets.[1] The combination of fibers and metals provides properties like tensile, flexural, impact, and damping, which can be controlled by the design and stacking scheme of the cored fiber materials.[2] Researchers have used three common configuration schemes for SCs, which are: 1) metal and fiber, 2) fiber and metal, and 3) interplaying a single fiber or multiple fiber layers between metal sheets.[3] In addition to these configurations, researchers have also alternately plied various fibers to improve SC properties, such as Jute (J) and high strength Basalt (K) layers between Ti sheets.[4] This configuration, termed as Sm/Ba/J/Ba/J/Sm SC, has been investigated for its ability to increase the internal dissipation of shock energy and tensile stre ngth of Sm SC.[5] It is expected that the fabricated Sm/Ba/J/Ba/J/Sm SC will be a cost-effective alternative to SCs based on carbon and aramid fibers.[6,7] The researchers in this study focused on the machining and secondary processing of SC materials, in addition to analyzing SC fabrication. They found that conventional methods for machining SCs are impractical due to the materials' heterogeneity and thermal sensitivity, resulting in significant damage during processing, such as cutting of holes.[8,9,10] This damage can cause dimensional and geometric deviations and stress concentrations around the holes, which can affect the performance of the SC and even lead to total failure.[11] The researchers propose exploring the feasibility of advanced machining processes, such as abrasive water jet cutting (AWJC), to avoid damage and produce high-quality SCs.[12] In summary, the literature suggests that AWJ machining is a promising technique for cutting holes in SCs, as it offers several advantages over conventional methods, such as flexibility, minimum cutting errors, and smaller cutting force.[13]

Moreover, previous studies have shown that AWJC machining can produce holes with minimum damage and high-quality surfaces in various composite materials, including polymer composites, graphite/epoxy composites, glass-fiber reinforced plastics, and carbon fiber-reinforced plastics.[14] Cutting is a commonly used machining method in the aerospace industry, accounting for 40% of all machining operations, particularly in assembling components and parts [15,16,17]. However, there is limited literature on the use of AWJC operations for cutting, milling, trimming, and turning of SCs made of steel mesh. Therefore, this study focuses on investigating the impact of AWJC variables on the cutting of Sm/Ba/J/Ba/J/Sm SC.

2. Materials and methods

The (W/B/J/B/J/W) WLA is a composite material made up of layers of steel mesh, basalt, and jute fiber. We selected it to investigate the effect of the three reinforcement layers on the process parameters of AWJM. With a working bed of 320 x 1700 cm & a table height of 91 cm, the AQUVAJET CNC machine has an A, B and C-axis movement of 300, 150 and 20 cm. The AP's 400 MPa ultimate operating pressure is developed by a 37 KW engine. During the cutting operation, neither the jet angle (90°) nor the aiming tube diameter (0.11 cm) changed. An injection-type nozzle with a 0.032 cm diameter was used. MITUTOYO SJ-210 equipment was used to conduct the SR measurements. The sample length was changed to 4 mm, the least count to 0.01 cm, & the cutoff 0.8 mm according to the profilometer's operating instructions. At the middle area of the cut, the SR values were estimated using an average of five measurements on each surface. The cut direction was used to take the measurements. The homogeneity of surface between the jet's entry & exit sites varies significantly, although these results are typical of the quality control of the AWJC cut surface. A fine jet of water with extremely high AJP & abrasive slurry is used to cut the target substance using erosion. Each AWJC surface had numerous spots where the surface undulation measurements were obtained, & the measurement's overall length covered the metal's top, middle, & bottom regions. Figure 1 shows the abrasive jet machine used for studies.

Figure 1. Abrasive water Jet Machine

2.1 Response surface methodology

In general, response surface methodology (RSM) is used to create a second-order mathematical polynomial equation, as shown in equation 1 and 2, which establishes a correlation between the variables involved in abrasive water jet cutting and the resulting machining responses of SC cutting. Response surface models were generated using Design Expert (V.12) software, with the AWJC variables and their inter-level ranges listed in Table 1. The selection of parameters and their levels was based on standard literature, which focuses on the abrasive water jet cutting and machining of various SC and polymer composites. A central composite design with five center point (29 experiments) sets were used to assess the SR, KA and MRR of machined SC, as shown in Table 2. Figure 2 depicts the predicted and actual value of SR, Ka and MRR. It indicates that the experimental

results & and the expected models are in agreement. Below are the mathematical equations (1, 2, 3) that have been coded.

Table 1. Levels of process parameters

Parameters	Unit	Level -2	-1	0	1	2
AFR	**g/min**	**170**	**220**	**270**	**320**	**370**
AJP	**MPa**	**100**	**150**	**200**	**250**	**300**
SOD	**mm**	**1.5**	**2**	**2.5**	**3**	**3.5**
TS	**mm/min**	**100**	**125**	**150**	**175**	**200**

Table 2. Experimental observations of SR and KA

Run order	AJP	SOD	TS	AFR	SR (µm)	KA	MRR (mm^3/sec)
1	200	2.5	150	220	4.32	1.68	4.717
2	300	1.5	100	370	2.79	1.18	5.418
3	200	2.5	150	270	4.09	1.59	5.307
4	200	2.5	150	270	4.09	1.59	5.307
5	100	3.5	200	370	4.58	1.72	3.883
6	300	1.5	200	170	3.51	1.45	5.212
7	100	1.5	100	170	4.62	1.75	2.532
8	200	2.5	125	270	4.01	1.55	5.135
9	100	3.5	100	370	4.23	1.62	3.895
10	250	2.5	150	270	3.78	1.52	5.894
11	300	1.5	100	170	3.21	1.36	4.121
12	300	3.5	200	170	3.64	1.47	6.479
13	200	2.5	175	270	4.25	1.63	5.621
14	100	3.5	200	170	5.08	1.85	3.742
15	300	3.5	200	370	3.31	1.37	6.957
16	100	1.5	100	370	3.73	1.51	3.269
17	150	2.5	150	270	4.34	1.71	4.428
18	200	2.5	150	270	4.09	1.59	5.307
19	200	2.5	150	270	4.09	1.59	5.307
20	200	2	150	270	4.02	1.57	5.102
21	300	3.5	100	370	3.11	1.27	6.532
22	200	2.5	150	320	3.91	1.53	5.647
23	200	3	150	270	4.27	1.63	5.938
24	100	1.5	200	170	4.91	1.83	2.841
25	300	1.5	200	370	3.01	1.24	6.285
26	200	2.5	150	270	4.09	1.59	5.307
27	100	1.5	200	370	4.13	1.61	3.662
28	100	3.5	100	170	4.78	1.81	3.398
29	300	3.5	100	170	3.47	1.42	6.009

Table 3. ANOVA table for SR

Source	Sum of Squares	df	Mean Square	F-value	p-value
Model	8.35	4	2.09	92.37	< 0.0001
AJP	6.42	1	6.42	283.88	< 0.0001
SOD	0.3535	1	0.3535	15.64	0.0006
TS	0.3347	1	0.3347	14.81	0.0008
AFR	1.25	1	1.25	55.14	< 0.0001
Residual	0.5425	24	0.0226		
Lack of Fit	0.5425	20	0.0271		
Pure Error	0	4	0		
Cor Total	8.89	28			

Table 4. ANOVA table for KA

Source	Sum of Squares	df	Mean Square	F-value	p-value
Model	0.7442	4	0.186	96.37	< 0.0001
AJP	0.5583	1	0.5583	289.19	< 0.0001
SOD	0.0241	1	0.0241	12.46	0.0017
TS	0.0264	1	0.0264	13.68	0.0011
AFR	0.1355	1	0.1355	70.17	< 0.0001
Residual	0.0463	24	0.0019		
Lack of Fit	0.0463	20	0.0023		
Pure Error	0	4	0		
Cor Total	0.7905	28			

Table 5. ANOVA table for MRR

Source	Sum of Squares	df	Mean Square	F-value	p-value
Model	32.62	4	8.16	40.38	< 0.0001
A-PRESSURE	25.53	1	25.53	126.42	< 0.0001
B-Standoff distance	3.85	1	3.85	19.08	0.0002
C-TS	1.03	1	1.03	5.12	0.0330
D-flow rate	2.21	1	2.21	10.92	0.0030
Residual	4.85	24	0.2019		
Lack of Fit	4.85	20	0.2423		
Pure Error	0.0000	4	0.0000		
Cor Total	37.47	28			

$$(SR)= +4.50 - 0.6801* (AP) + 0.1588* (ND) + 0.1532* (TR) - 0.2962* (MSR) \quad (1)$$

$$(KA) = + 1.99 - 0.3047* (AP) + 0.0694* (ND) + 0.0767* (TR) - 0.1356* (MSR) \quad (2)$$

$$MRR= +4.76+1.24 *(AP)+ +0.4832* (ND) +0.2503 *(TR) +0.3656 *(MSR) \quad (3)$$

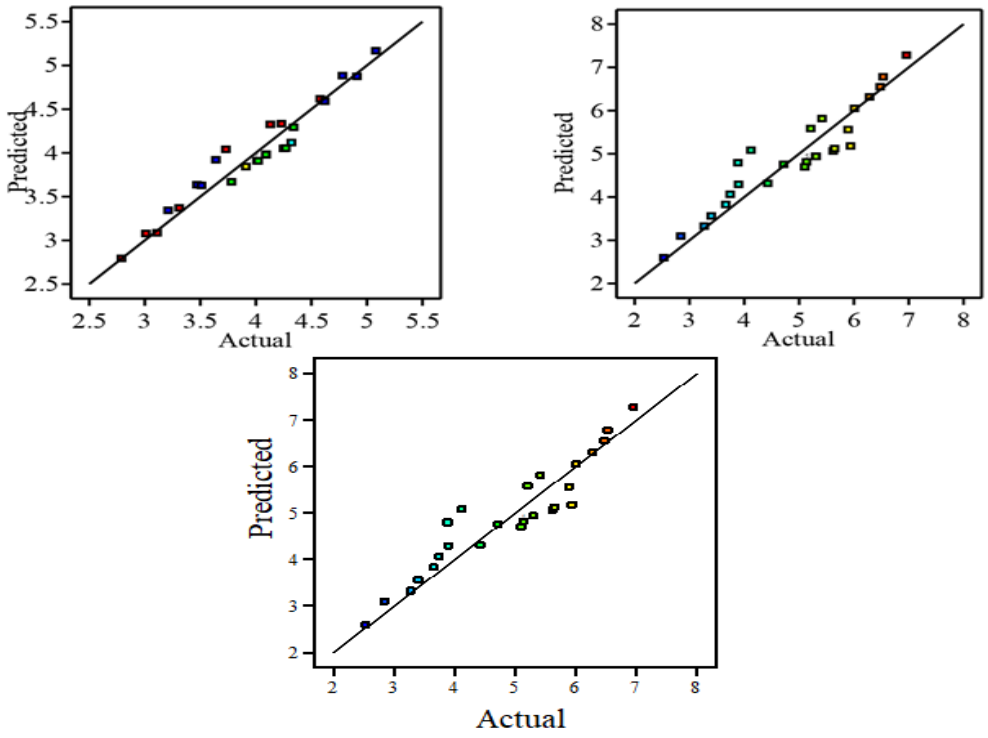

Figure 2 Comparison between predicted and experimental values SR, KA, and MRR

3. Results and discussion

3.1 Surface roughness (SR)

It is vital to study the quality of AWJC materials surface, particularly SC, to predict how the components will interact with surrounding essentials & various operating conditions. With the use of 3D plots, the overall effect of AWJC factors on the SR is visualized graphically in Fig. 3. The SR value was at its lowest at a more substantial pressure of 300 MPa, as shown in Fig. 3(a). However, the variation of SR reaches a greater value of 3.31 µm when the levels of AP & TR are low & high, respectively. On the other hand & dropping the TR from 200 to 100 mm/min produced a minimal value of 2.51 µm while keeping the AJP's set point high. The SU variation in the AJP 100-300 MPa range was investigated using a mid-range of other parameters. When the AP was intensifies from 100 to 300 MPa, the SR reduced by 10.51%. Thus, an intensifies in AJP may intensifies the kinetic energy of the aqua stream & result in a high-energy state transition for the abrasive bits. Therefore, regardless of the secular state, tremendous energy abrasive particles travelling through a cut zone cause less snagging & more constant erosion together with the material's thickness. In contrast hand, a rise in AJP causes SR to decrease significantly. When the TS was boosted from 20 to 60 mm/min, the SR intensified by 9.14%. The overlap between the aqua jet's subsequent motions is the shortest. In the cutting zone, traverse rates for coarse particles per unit area appear to be ultimate as a result. This causes the cutting component to be roughly machined, often producing a more uneven surface. With rising SOD & TS, the SR reached 4.668 µm, as illustrated in Fig. 3 (b). The influence of SOD on SR was examined in different range with an AFR of 320 g/min, AJP of 250 MPa, & TS of 40 mm/min (middle level). When the SOD was intensifies from 1.5 to 3.5 mm, the SR intensified by 6.75%. Roughing, for instance, is brought on by an intensifies in SOD in SC. A sliced surface that has a minimum grade of ND could be smoother. At a greater AFR of 320 g/min, which converts to 320 g/min, the SR value is low as shown in Fig. 3 (c). With a parametric AFR of 320 g/sec & a AJP of 300 MPa, the minimal value 3.08 µm. It's crucial to remember that the SR fell by 10.41% as the AFR intensifies from a low to a high value. This is because

a ultimate AFR makes more abrasive particles accessible. In other words, the amount of grinding particles travelling over the cutting zone improves the random cutting on SC. Because of this, it causes erosion to be more constant at more extended depths, producing a surface that is smooth cut & has less SR.

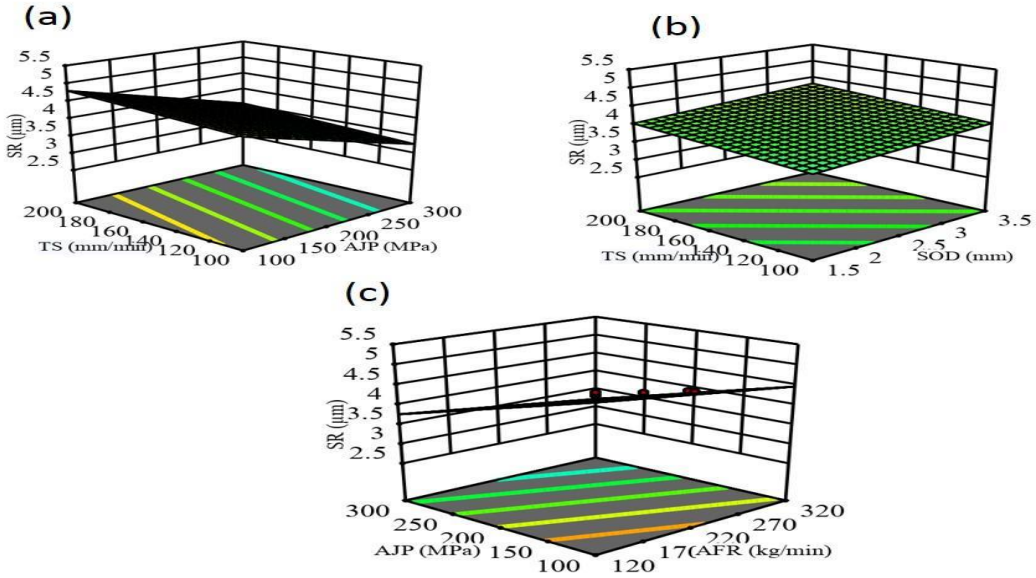

Figure 3 3D plot and interaction of SR

3.2 Kerf angle (KA)

With the use of 3D plots, the overall effect of AWJC factors on the KA is visualized graphically in Fig. 4. The KA fluctuation, however, rises to a ultimate value of 2.345 degrees when AJP & TS levels are low & high, respectively. When the TS was minimul from 200 to 100 mm/min, the KA was dropped to 1.12 degrees. Keep the AJP's setting at a ultimate level, however. The KA fluctuation was examined in the AJP 100-300 MPa range with constant mid-level of other parameters. When the AJP was intensifies from 150 to 350 MPa, the KA diminished by 21.25%. This might result from the hydraulic set height increasing linearly with AJP. Consequently, a gap develops at the material's thickness closest to the jet's diameter. As a result, the KA in the cutting zone of the workpiece is relatively constant. Additionally, the SC found that raising the pressure almost had the same KA result from top to bottom.

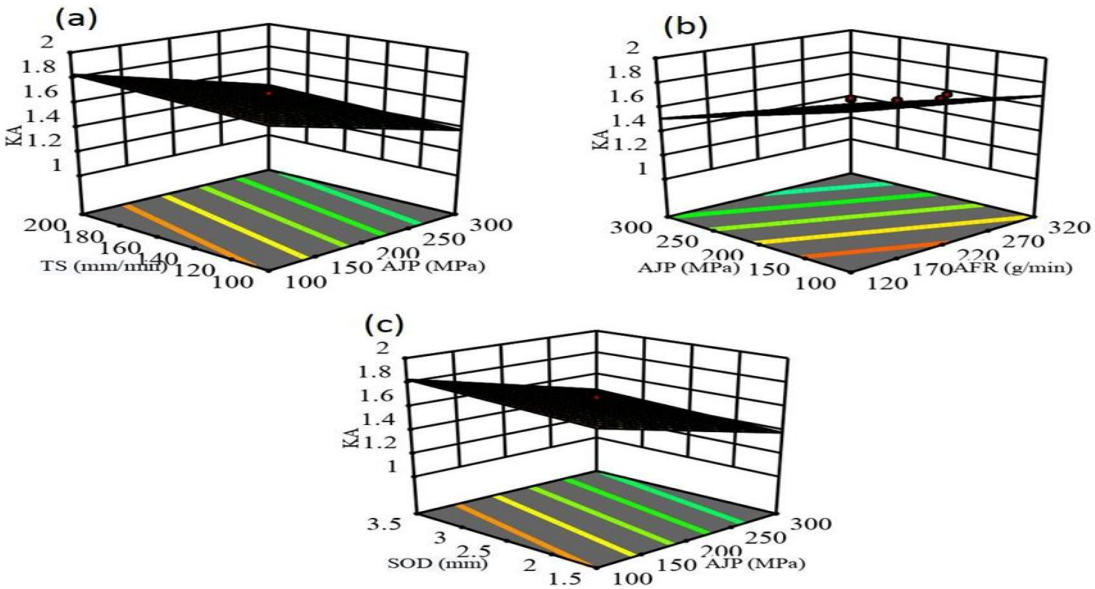

Figure 4 3D plot and interaction of KA

To show how the nozzle distance affects cutting behavior, the nozzle distance was intensifying from 1-3 mm while keeping other variables at mid-level. With a 6.25% intensifies in the KA, the SOD was intensifying from 1.5 to 3.5 mm. This might be because the aqua jet is moving away to orifies, decreasing its width & partially converting some of its velocity into grinding particles. In an aqua jet, abrasive particles lose some life & processing capacity. Penetrating ability is thereby diminished. The bottom KA is thus lesser than the top KA. As a consequence, at greater SOD levels, the KA was bigger.

The AFR was set to 320 g/sec, & the interaction parameter was adjusted to 150 MPa, as illustrated in Fig. 4 (b), where the KA was at its ultimate. AFR was analyzed with of 120 - 320 g/sec at mid-range of other parameters. The KA rose by 11.52% when the AFR dropped from 320 to 120 g/sec. The bottom notch converts smaller due to the short machining times; it unequivocally establishes that the AFR directly affects the KA. According to Fig. 4 (c), the ultimate KA of 2.450 was reached at a high SOD & low AJP. After increasing SOD & AJP, KA diminished to 0.580. SOD is altered from 3 to 1 mm while mid-level of others factors to ascertain the effect of SOD on KA. When the SOD steadily dropped from 3 to 1 mm, the KA diminished to 9.18%.

3.3 Material Removal Rate (MRR)

In Fig. 5, the overall impact of AWJC parameters on the MRR is graphically represented using 3D plots. However, when AJP and TS levels are high, respectively, the MRR fluctuation increases to a maximum value of 6.285 mm3/sec. The MRR rose when the TS reached its maximum at 100 to 200 mm/min, as seen in Fig. 5 (a). Further increase in the width of the beam is noticed with a change in SOD. At low AJP the rate of increase of MRR is low with respect to SOD in Fig. 5 (b). AJP and SOD surface plot in Fig. 5 (b), shows that MRR of SC increase on increase in SOD, where an increase in MRR is observed with increase in AJP. As shown in Fig. 5 (b), where the MRR was at its maximum, the AFR was set to 320 g/min, and the interaction parameter was changed to 300 MPa.

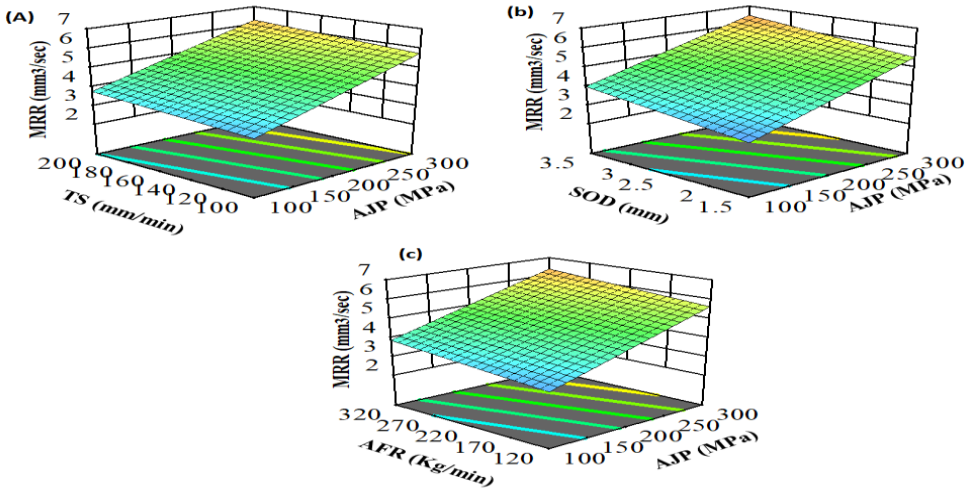

Figure 5 3D plot and interaction of MRR

3.3 Desirability approach optimization and validation

3.3.1 Desirability analysis (DA)

By assessing input factors, including AJP, SOD, TS, & AFR, the objective is to decrease AWJC responses of SR, KA and MRR. Equation (4) shows how this method translates process results to the necessary desirability value. To identify the best solutions by the constraints of the inputs, ultimate desirability values for the minimum response criteria were considered. The desired perturbation curves for (W/B/J/B/J/W) stacking composite in AAJC responses are shown in Fig. 6 (a).

$$d_f = [\frac{Max_i - R_i}{Max_i - Min_i}] \quad (4)$$

Max_i is the ultimate outcome value, & the mini is the response's minimum value.

R_i is the relative value of the trail response, & Wi is the response's weightage.

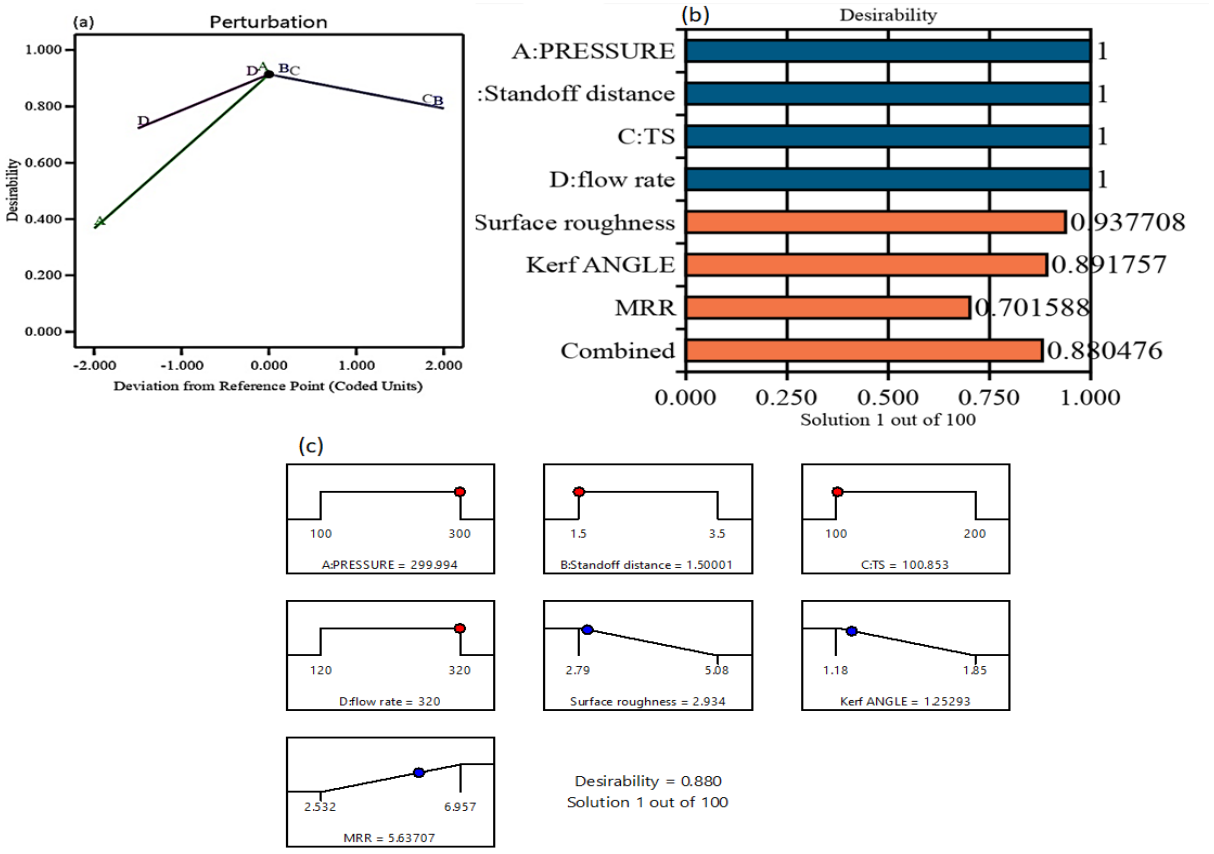

Figure 6 (a, b & c) Perturbation, Bar graph & Ramp

This plot displays the response area produced by the RSM technique. These curves show how, although the other variables remain constant, each variable's normal trend changes as it travels away from the point. The crucial characteristics of the RSM are also shown in this graph. When pressure and MRR intensify from a reference location, the perturbation graph reveals that SR and KA decreased. When these two factors were contrasted, AJP emerged as the essential factor in attaining the expected output responses. On the other hand, SR grew considerably, whereas SOD & TR climbed from a baseline to KA According to how they affect the objective, the process variables are ranked by the perturbation diagram as follows: (AJP) > (AFR) > (SOD) > (TS). The desirability analysis graph in Fig. 6 (b) displays the relative desirability range of responses. A desirability is closer to 1 was chosen to demonstrate how process variables like SR & KS reduction impact the accuracy of the goal solution. The desirability range of TS, AJP, SOD, & AFR on the desirability bar graph was equal to 1, showing that all elements met the requirements. According to Fig. 6, the ramp function forecasts the ideal values. The essential parameters for attaining the Maximum MRR and lowest SR, KA are SOD= 1.5. mm; AJP= 300 MPa, TS= 100 mm/min, & AFR= 320 g/sec.

To provide the ideal circumstances for AWJC of SC, Fig. 6 (a-c) is utilized to validate the relationships among variables & and outcomes. More uniform erosion caused by high AJP & AFR values produced a smoother surface & a narrow kerf.

3.4 Experimental validation

Confirmatory tests were carried out to compare the experimental findings in Table 4 with those predicted by the RSM models. As a result, the RSM created for AAJC on stacking composite are suitable, as shown by the validation studies showing a less than 5%.

Table 6 Validation

SOD (mm)	AJP (MPa)	TS (mm/min)	AFR (g/sec)	Predict			Actual			Error%		
				SR	KR	MRR	SR	KR	MRR	SR	KR	MRR
1.5	100	100	220	2.93	1.25	5.56	2.89	1.23	5.57	1.36	1.6	1.07
2.5	200	150	270	3.13	1.28	5.58	3.19	1.26	5.51	1.91	1.56	1.24
3.5	300	200	370	3.15	1.32	5.49	3.21	1.35	5.42	2.53	2.27	1.27

4. Conclusions

AWJC has been used to machine (W/B/J/B/J/W) stacking composite utilizing a variety of parameters, including AJP, SOD, TS, & AFR. It was decided to combine RSM optimization with DA to discover essential process factors & and their connections to cutting features.

1. To investigate the relative relevance of variables when minimizing, SR and KA ANOVA statistics are used. The most important factor, which accounted for 73% of the SR and 74% of the KA, was the pressure of the abrasive aqua jet. The AFR, SOD, and TS were additional process variables with a negligible effect.
2. The experimental findings show that raising the AJP reduces SR and KA. Due to its ultimate vitality and the fact that it intensifies the AFR of abrasive particles per unit time, the (Sm/Ba/J/Ba/J/Sm) stacking composite degrades more evenly throughout the aqua jet's penetration line. On the other hand, it was found that the other two factors, TS and SOD, had the opposite impact on the KA, SR and MRR of the machined component.
3. The aqua jet loses energy due to the jet boundary diverging with increasing SOD, severely limiting the amount of material machined in the (Sm/Ba/J/Ba/J/Sm) stacking composite core region. In addition, a minimal aqua jet overlap and cutting time are also caused by intensified TS.
4. The RSM approach improved the AWJC factors of AP 300 MPa, TR 100 mm/min, SOD 1.5 mm, & AFR 320 g/sec to decrease SR & KA values. AJP > AFR > SOD>TS, the AWJC attractiveness analysis variables also showed TR in their proportional effect on machining excellence characteristics. RSM-predicted SR, KA, and MRR values models are validated using experimental data, demonstrating that they agree with one another with minimal error.

References

[1] Arpatappeh FA, Azghan MA and Eslami-Farsani R. The effect of stacking sequence of basalt and Kevlar fibers on the Charpy impact behavior of hybrid composites and fiber metal laminates. *Proc. Inst. Mech. Eng. Part C J. Mech. Eng. Sci* 2020; 234: 3270-9.

[2] Chandrasekar M, Ishak MR, Jawaid M, et al. An experimental review on the mechanical properties and hygrothermal behaviour of fibre metal laminates. *J. Reinf. Plast. Compos.* 2017; 36: 72-82.

[3] Salve A, Kulkarni R and Mache A. A Review: Fiber Metal Laminates (FML's) - Manufacturing, Test Methods and Numerical Modeling. *Int. J. Eng. Technol. Sci* 2016; 6: 71-84.

[4] Kali N, Pathak S and Korla S. Effect on vibration characteristics of fiber metal laminates sandwiched with natural fibers. *Mater. Today Proc* 2020; 28: 1092-6.

[5] Prabhakaran S, Krishnaraj V and Zitoune R. Sound and vibration damping properties of flax fiber reinforced composites. *Procedia Eng* 2014; 97: 573-81.

[6] Prabhakaran S, Krishnaraj V, Shankar K, et al. Experimental investigation on impact, sound, and vibration response of natural-based composite sandwich made of flax and agglomerated cork. *J. Compos. Mater.* 2020; 54: 669-80.

[7] Ramraji K, Rajkumar K and Sabarinathan P. Mechanical and free vibration properties of skin and core designed basalt woven intertwined with flax layered polymeric laminates. *Proc. Inst. Mech. Eng. Part C J. Mech. Eng. Sci* 2020; 234: 4505-19.

[8] Bañon F, Sambruno A, González-Rovira L, et al. Review on the Abrasive Water-Jet Machining of Metal-Carbon Fiber Hybrid Materials. *Metals* 2021; 11: 164.

[9] Dong S, Liao W and Zheng K, Ma W. Investigation on thrust force in rotary ultrasonic drilling of CFRP/aluminum stacks. *Proc. Inst. Mech. Eng. Part C J. Mech. Eng. Sci* 2020; 234: 394-404.

[10] Bayraktar S and Turgut Y. Determination of delamination in drilling of carbon fiber reinforced carbon matrix composites/Al 6013-T651 stacks. *Measurement* 2020; 154: 107493.

[11] Jia Z, Chen C, Wang F, et al. Experimental study on drilling temperature and hole quality in drilling of carbon fiber reinforced plastic/titanium stacks. *Proc. Inst. Mech. Eng. Part C J. Mech. Eng. Sci* 2020; 234: 2662-72.

[12] Xu J, Li C, Chen M, et al. On the analysis of temperatures, surface morphologies, and tool wear in drilling CFRP/Ti6Al4V stacks under different cutting sequence strategies. *Compos. Struct.* 2020; 234: 111708.

[13] Kuo C, Li Z and Wang C. Multi-objective optimization in vibration-assisted drilling of CFRP/Al stacks. *Compos. Struct.* 2017; 173: 196-209.

[14] Kumar D, Gururaja S and Jawahir IS. Machinability and surface integrity of adhesively bonded Ti/CFRP/Ti hybrid composite laminates under dry and cryogenic conditions. *J. Manuf. Process* 2020; 58: 1075-87.

[15] Vijayakumar R, Srirangarajalu N, Santhanakumar M, Edwin Paul N E, Rajesh M. Investigation of Abrasive Aqua Jet Hole Making (AAJHM) parameters using desirability analysis on Inconel-625 space alloy. J Manuf Process. 2023; 92: 311-328.

[16] Pawar OA, Gaikhe YS, Tewari A, et al. Analysis of hole quality in drilling GLARE fiber metal laminates. Compos. Struct. 2015; 123: 350-65.

[17] Srirangarajalu N, Vijayakumar R, Rajesh M. Multi-performance investigation of Inconel-625 by abrasive aqua jet cutting. Mater. Manuf. Process. 2021, 1–12.